SAND2019-4788C

Performance Evaluation of STATCOM Equipment using Ambient and Disturbance Data

Christoph Lackner
Rensselaer Polytechnic Institute
Troy, NY, US

Joe H. Chow
Rensselaer Polytechnic Institute
Troy, NY, US

Felipe Wilches-Bernal
Sandia National Laboratories
Albuquerque, NM, US

***Abstract*—With increasing availability of synchrophasor technology, enabled by phasor measurement units (PMUs), applications based on this technology are being implemented as a practical approach for power systems monitoring and control. While synchrophasor data provides significant advantages over SCADA data it has limitations especially in the area of model validation and estimation. With the increasing complexity of the power system, the need for equipment monitoring and performance evaluation becomes more relevant. Traditionally model validation and estimation process can be used to look at control equipment performance. However, due to the challenges associated with these processes there are limitations on the performance evaluation. This work expands a previously introduced algorithm to monitor control system performance to allow the algorithm to work under power system ambient and disturbance conditions. Additionally the algorithm is demonstrated on data obtained from the interconnection point of a STATCOM device during ambient and disturbance operation.**

I. Introduction

Synchrophasor technology, enabled by phasor measurement units (PMUs), is now prevalent in power systems around the world. Applications based on this technology such as state estimation are being implemented as a practical approach for power systems monitoring and control [1], [2]. PMUs also provide much higher data resolution than traditional SCADA measurements. This allows the data to be used for a variety of equipment monitoring and evaluation purposes, such as model validation and performance monitoring [3].

A significant amount of work has been done using PMU data for dynamic state estimation; in [4] this approach is used for synchronous generator model validation and identification. While PMUs nominally report data at 30, 50 or 60 samples per second, most generator model calibration algorithms require much higher sampling rates [4]. This means PMUs with higher resolution need to be installed to monitor and evaluate detailed generator control system performance.

This research was in part supported by the Engineering Research Center Program of the National Science Foundation and the Department of Energy under NSF Award Number EEC-1041877, NSF Award Number EEC-1550029, the CURENT Industry Partnership Program and NYSERDA under Award Number PON-3397.

Sandia National Laboratories is a multimission laboratory managed and operated by National Technology and Engineering Solutions of Sandia, LLC, a wholly owned subsidiary of Honeywell International, Inc., for the U.S. Department of Energy's National Nuclear Security Administration under contract DE-NA0003525.

This research was supported in part by the U.S. Department of Energy Transmission Reliability program.

The work in [5] introduces a low-order dynamic model of a generator to estimate and monitor generator control system performance without requiring higher sampling rates. The work also proposes an initial algorithm to use disturbance data taken at the point of interconnection to monitor the control system performance. This paper introduces an enhanced version of that algorithm to monitor the control performance of a STATCOM using synchrophasor data taken at the point of interconnection. Unlike the original algorithm introduced in [5] the enhanced algorithm proposed in this paper does not rely only on disturbance data, but is capable of using ambient data without any power system disturbance content.

The proposed algorithm is capable of identifying control system performance based on the small changes in steady state operating condition of the power system due continuous load changes and changes in generation equipment outputs. Because synchronous generator control equipment such as exciters and governors often do not act on such small changes due to controller deadbands, it is extremely difficult to monitor their performance under ambient conditions. However, Flexible AC Transmission System (FACTS) devices such as a STATCOM continuously operate without deadbands and react to small changes, allowing the proposed algorithm to monitor performance almost continuously [6].

The remainder of this paper is organized as follows. Section II introduces a dynamic model of a STATCOM. Section III introduces the enhanced algorithm proposed in this work. Section IV contains the performance evaluation results of the STATCOM using disturbance data. Section V contains the performance evaluation results using ambient data, and finally Section VI concludes the paper.

II. STATCOM

This section introduces a STATCOM and the dynamic model used in most power system simulations [6]. A STATCOM is a voltage- sourced converter based FACTS device that can inject reactive current into the network to support the voltage at its terminal bus. Figure 1 shows the connection diagram of a STATCOM.

Figure 2 shows the terminal voltage vs the injected current of the STATCOM under normal operations with droop control. Figure 3 shows a dynamic model of a STATCOM [7]. Based on this dynamic model and given the voltage error

$$V_{\mathrm{err}} = V_{\mathrm{ref}} - V_{\mathrm{T}} \tag{1}$$

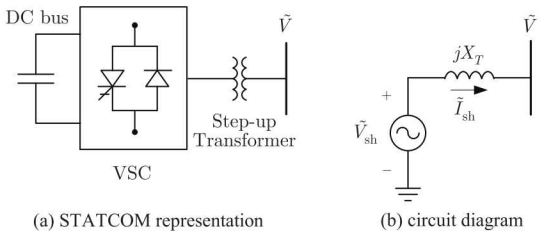

(a) STATCOM representation (b) circuit diagram

Fig. 1. Connection diagram of a STATCOM

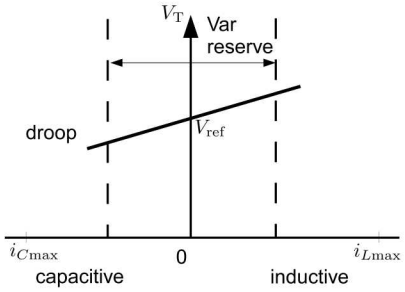

Fig. 2. STATCOM operation in droop control

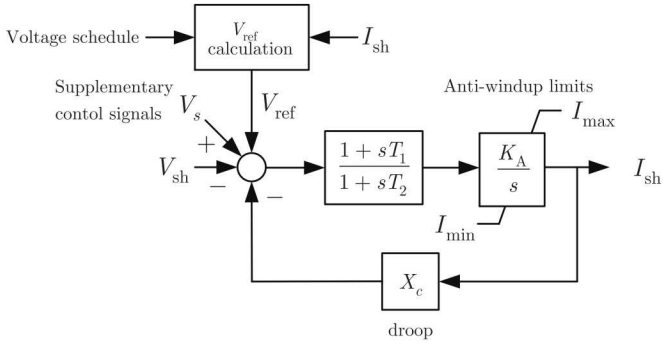

Fig. 3. Dynamic model of a STATCOM

where $V_{\rm T}$ is the terminal voltage indicated by $V_{\rm sh}$ in Figure 3. The reactive output current can be written as

$$I_{\rm sh} = \frac{(1+sT_2)s}{1+s(T_1K_A+X_C)+s^2X_cT_1}V_{\rm err} \tag{2}$$

Assuming a constant voltage schedule and $V_{\rm ref}$, no supplemental control signal $V_{\rm s}$, and $T_1 \approx T_2$ [8] this can be simplified to

$$I_{\rm sh} = \frac{1}{K_A+sX_C}V_{\rm err} = \frac{\frac{1}{K_A}}{1+s\frac{X_C}{K_A}}V_{\rm err} \tag{3}$$

Note that this simplified model is very similar to the simplified voltage control model introduced in [9] and [5].

III. Enhanced Performance Monitoring Algorithm

Figure 4 shows the original performance estimation algorithm proposed in [5]. The first 2 stages involve some

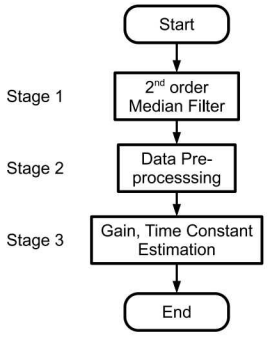

Fig. 4. Algorithm to obtain estimated dynamic model

data pre-processing to remove any noise and the DC bias component. The proposed enhancement in this paper replaces these two stages with a PMU signal separation algorithm, which is designed to separate the signal into a 3 distinct components representing the quasi-steady state (QSS), the dynamic component of the signal and the noise component. Section III-A describes this proposed signal separation in more detail.

The proposed enhancement also improves the time constant and gain estimation in stage 3 by taking into account the relative weight of each parameter and adjusting accordingly the numerical optimization. Section III-B describes those adjustments in more detail.

A. Signal Separation Algorithm

For the purpose of this analysis, any PMU signal is considered a summation of 3 components:

$$x(t) = x_{\rm qss}(t) + x_{\rm d}(t) + x_{\rm n}(t) \tag{4}$$

where $x_{\rm qss}(t)$ represents the QSS component, $x_{\rm d}(t)$ is the dynamic component and $x_{\rm n}(t)$ is the noise component of the signal [10]. By considering a signal without any noise such as

$$y(t) = y_{\rm qss}(t) + y_{\rm d}(t) \tag{5}$$

the QSS component and dynamic component can be explained in more detail.

Figure 5 shows such an ideal signal $y(t)$ and its QSS component. In a power system the QSS represents the changes in the steady state operating conditions due to changes in the load or generation setpoints. During normal operation this component is composed of the slow parts of the signal. During disturbances such as generation trips the operating point of the system can change rapidly and the QSS component also contains some faster parts of the signal. Figure 6 shows another example of an ideal signal without noise during a generation trip and its QSS component.

Figure 7 shows the dynamic component of these two examples. This component is due to the synchronous generators and control equipment interacting in the system. This components contains parts of the electromechanical swings and parts of faster oscillations present in the signal.

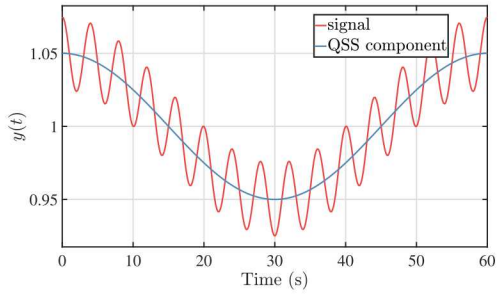

Fig. 5. Ideal signal during steady state operation

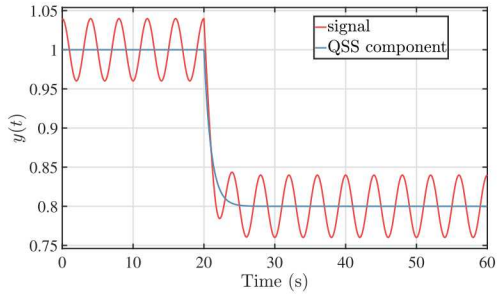

Fig. 6. Ideal signal during power system disturbance

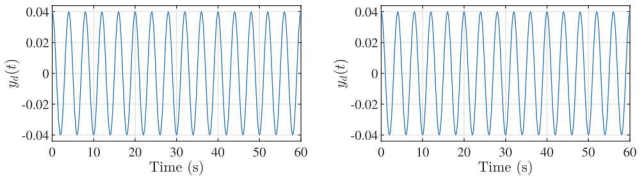

(a) during steady state operation (b) during power system disturbance

Fig. 7. Dynamic component of the ideal signal

Figure 8 shows the algorithm used to separate these 3 components from the original signal. Initially, a median filter is applied to remove individual outliers due to issues in the PMU phasor computation [11]. The resulting signal is then passed through a low-pass filter of the form

$$x_{\mathrm{lpf}}[k] = \frac{a_0 x_{\mathrm{med}}[k] + a_1 x_{\mathrm{med}}[k-1] + a_2 x_{\mathrm{med}}[k-2]}{b_1 x_{\mathrm{lpf}}[k-1] + b_2 x_{\mathrm{lpf}}[k-2]} \quad (6)$$

with

$$a_0 = 0.0744 \qquad a_1 = 0.1487 \qquad a_2 = 0.0744$$
$$b_1 = 0.1487 \qquad b_2 = 0.3919$$

This filter removes any high frequency noise that is present in the signal. Then a first-order empirical mean decomposition (EMD) is used to remove the QSS component, a step similar to stage 2 of the algorithm in 4 [5]. The EMD estimates an upper and lower envelope of the signal similar to that seen in Figure 9. The first part of the QSS component is computed by

$$x_{\mathrm{qss}\ 1}(t) = \frac{x_{\mathrm{upper}}(t) + x_{\mathrm{lower}}(t)}{2} \quad (7)$$

the remaining part of the signal is passed through a high-pass filter of the form

$$x_{\mathrm{hpf}}[k] = \frac{a_0 x_{\mathrm{emd}}[k] + a_1 x_{\mathrm{emd}}[k-1] + a_2 x_{\mathrm{emd}}[k-2]}{b_1 x_{\mathrm{hpf}}[k-1] + b_2 x_{\mathrm{hpf}}[k-2]} \quad (8)$$

with

$$a_0 = 0.9767 \qquad a_1 = -1.9534 \qquad a_2 = 0.9767$$
$$b_1 = -1.9529 \qquad b_2 = 0.9540$$

This additional filtering removes any remaining slow frequency DC-bias components that are not part of $x_{\mathrm{qss}\ 1}(t)$. Finally, the three components are computed as

$$x_{\mathrm{qss}}(t) = x_{\mathrm{qss}\ 1}(t) + (x_{\mathrm{emd}}(t) - x_{\mathrm{hpf}}(t)) \quad (9)$$
$$x_{\mathrm{d}}(t) = x_{\mathrm{hpf}}(t) \quad (10)$$
$$x_{\mathrm{n}}(t) = x(t) - x_{\mathrm{qss}}(t) - x_{\mathrm{d}}(t) \quad (11)$$

where $x_{\mathrm{emd}}(t)$ and $x_{\mathrm{hpf}}(t)$ are the signals after the EMD and the high-pass filter are applied, respectively. The remainder of the performance estimation algorithm uses only the dynamic component of the signal. However, other PMU data applications such as fault identification [12] or cyberattack detection could potentially use the other components of the signal.

B. Time Constant and Gain Estimation

In [5] a simple algorithm to estimate the parameters of (2) is to minimize the squared-error function

$$J = |I_q - H(s) \star V_T|^2 \quad (12)$$

where

$$H(s) = \frac{K}{Ts+1} \quad (13)$$

However, an issue raised in [5] is that the resulting time constants vary significantly. Further analysis of this issue has shown that a change in K has a significant effect on J while a similar change in T has a much smaller effect. Therefore any numeric optimization such as those in [13] will result in K converging to a consistent value while the final value T is dependent on the initial guess and the number of iterations in the numeric optimization.

In order to make the time constant obtained more consistent over the various data windows, a 2-step optimization approach is proposed. Initial values for K and T are obtained by optimizing (12) using (13) with both K and T as adjustable parameters. In a second step (12) is optimized with only T as an adjustable parameter and K set to the value found in the previous step. This approach has proven effective in increasing the consistency in the estimation of T for similar datasets.

IV. Disturbance Data Results

This section contains some results obtained on the performance of a 200 MW STATCOM using the proposed algorithm based on historic PMU measurements during power system disturbances. Figure 10 shows the voltage and reactive current output of the STATCOM during one of the events. Figures 10a and 10c show the raw PMU signal as well as its QSS components. Figures 10b and 10d show the noise component

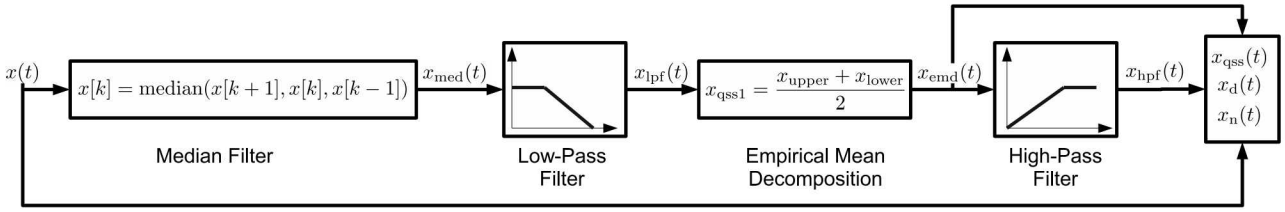

Fig. 8. Flowchart of the proposed signal separation algorithm

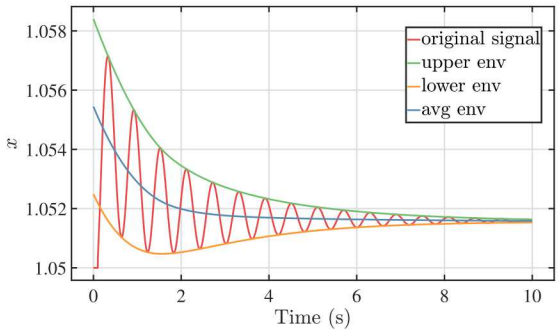

Fig. 9. Empirical Mean Decompositions (EMD) of an example signal

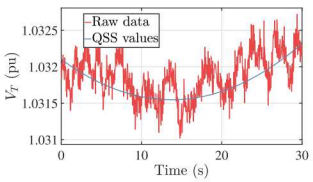

(a) Voltage signal and QSS component

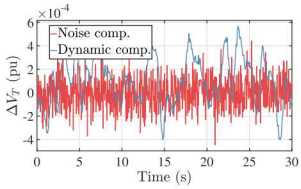

(b) Voltage noise and dynamic component

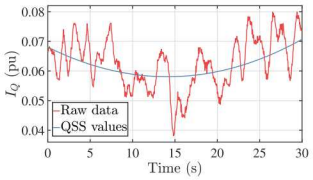

(c) Reactive output signal and QSS component

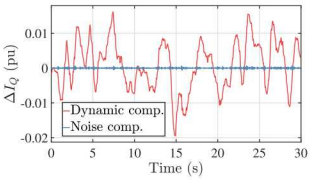

(d) Reactive output noise and dynamic component

Fig. 10. Signal separation results during disturbance

as well as the dynamic component which is then used to evaluate the STATCOM's performance.

Figures 11a and 11b show the voltage control performance using the full signal as and only the dynamic component of the signal respectively. While during the disturbance the full signal shows the droop reasonably well, the dynamic component shows the droop more clearly.

Table I contains the estimated droop and time constants for 16 disturbance events. The droop is between 2.70% and 4.36% in all cases, which indicate the STATCOM was performing similarly during all disturbances. The time constant is between 14.08 ms and 55.57 ms in all cases. The droop has a mean

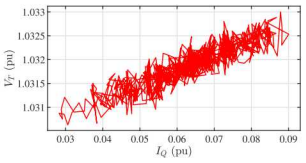

(a) using pre-processed signals

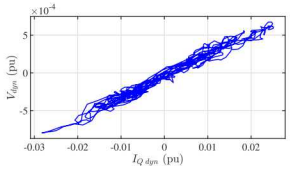

(b) using only dynamic component

Fig. 11. STATCOM voltage control performance during disturbance

TABLE I
DISTURBANCE DATA RESULTS

Disturbance	Droop (%)	T_{QV} (ms)
1	2.70	23.28
2	2.81	14.83
3	3.53	14.08
4	3.50	22.54
5	2.89	18.04
6	4.36	55.57
7	3.54	17.73
8	3.19	24.07
9	2.74	30.23
10	3.64	20.15
11	3.18	37.86
12	2.87	24.13
13	3.04	36.89
14	3.16	10.35
15	2.94	31.85
16	2.94	43.88

of 3.19% and a variance of $\sigma = 0.189\%$. The time constant has a mean of 26.59 ms and a variance of $\sigma = 146.94$ ms. Due to the fast nature of the power electronic interface of the STATCOM the time constant is relatively small and can't be estimated more accurately using the synchrophasor data.

V. AMBIENT DATA RESULTS

This section contains some results using the proposed method on ambient data sets. Figure 12 shows the voltage and reactive current output of the STATCOM during normal operation. Figures 12a and 12c show the raw PMU signal as well as the QSS components of the signals. Figures 12b and 12d show the noise component as well as the dynamic component which is then used to evaluate the STATCOM performance. While the dynamic component of the signals is very similar to that in Section IV, the QSS component is different since there is no large voltage change due to a disturbance.

Figure 13 shows the voltage control performance using the full signal as well as using only the dynamic component of

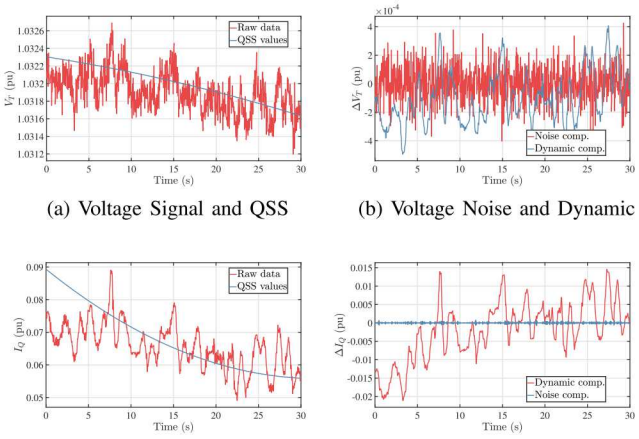

(a) Voltage Signal and QSS (b) Voltage Noise and Dynamic

(c) Reactive Output Signal and QSS (d) Reactive Output Noise and Dynamic

Fig. 12. Signal separation results during ambient operation

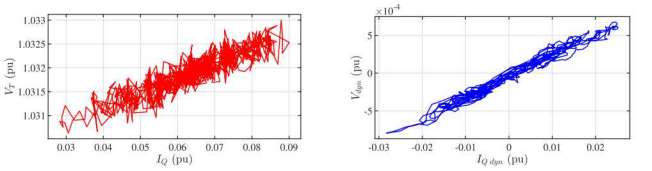

(a) using pre-processed signals (b) using only dynamic component

Fig. 13. STATCOM voltage control performance during ambient operation

the signal. During the ambient operation the action of the STATCOM is quite enough, which makes it is very difficult to see in the full signal. In the dynamic component it is still visible.

Table II contains the estimated droop and time constants for 14 ambient data sets. The droop is between 2.63% and 3.81% in all cases, which indicates the STATCOM was performing similar to the disturbance in Section IV. The droop has a mean of 3.14% and a variance of $\sigma = 0.148\%$. Similarly, the estimated time constants are between 11.04 ms and 44.76 ms with a mean of 28.50 ms and a variance of $\sigma = 99.65$ ms.

TABLE II
AMBIENT DATA RESULTS

Disturbance	Droop (%)	T_{QV} (ms)
1	3.24	11.04
2	3.07	35.13
3	2.96	32.71
4	3.19	24.80
5	2.63	14.10
6	3.22	21.78
7	2.95	38.38
8	3.17	38.44
9	2.36	44.76
10	3.39	30.83
11	3.05	18.77
12	3.80	26.85
13	3.10	24.01
14	3.81	37.38

Figures 12 and 13 show 30 seconds of ambient data, which is taken shortly before the disturbances in shown in Figure 10. Due to some missing data issues it was not possible to take ambient data before all 16 disturbances.

VI. CONCLUSIONS

This paper introduces an EMD-based algorithm to estimate a simplified dynamic model of a STATCOM based on the point of interconnection measurements. The estimated dynamic model can be used to evaluate the performance of STATCOM compared to historical performance and identify any changes in control system parameters.

The work includes some historic results based on disturbance data as well as ambient data. The results obtained using ambient data match the results obtained during disturbance events reasonable well. Since ambient data is constantly available this greatly improves the usefulness of this algorithm.

REFERENCES

[1] S. G. Ghiocel, J. H. Chow, G. Stefopoulos, B. Fardanesh, D. Maragal, B. Blanchard, M. Razanousky, and D. B. Bertagnolli, "Phasor-Measurement-Based State Estimation for Synchrophasor Data Quality Improvement and Power Transfer Interface Monitoring," *IEEE Transactions on Power Systems*, vol. 29, no. 2, pp. 881–888, March 2014.

[2] C. Lackner, Q. Zhang, and J. H. Chow, "Real-Time phasor-only state estimation with topology processing as OpenPDC adapter," in *2017 IEEE Power Energy Society General Meeting*, July 2017, pp. 1–5.

[3] Y. Li, R. Diao, R. Huang, P. Etingov, X. Li, Z. Huang, S. Wang, J. Sanchez-Gasca, B. Thomas, M. Parashar, G. Pai, S. Kincic, and A. Ning, "An innovative software tool suite for power plant model validation and parameter calibration using PMU measurements," in *2017 IEEE Power Energy Society General Meeting*, July 2017, pp. 1–5.

[4] L. Sun, A. P. S. Meliopoulos, Y. Liu, and B. Xie, "Dynamic state estimation based synchronous generator model calibration using PMU data," in *2017 IEEE Power Energy Society General Meeting*, July 2017, pp. 1–5.

[5] C. Lackner, J. H. Chow, and F. Wilches-Bernal, "Estimation of Generator Control System Performance using Synchrophasor Data," in *XIV Sepope*, September 2018, pp. 1–12.

[6] N. G. Hingorani, L. Gyugyi, and M. El-Hawary, *Understanding FACTS: concepts and technology of flexible AC transmission systems*. IEEE press New York, 2000, vol. 1.

[7] J. H. C. et al., *Power System Modeling, Computation, and Control*. IEEE press New York, 2019, vol. 1.

[8] X. Jiang, X. Fang, J. H. Chow, A. Edris, E. Uzunovic, M. Parisi, and L. Hopkins, "A Novel Approach for Modeling Voltage-Sourced Converter-Based FACTS Controllers," *IEEE Transactions on Power Delivery*, vol. 23, no. 4, pp. 2591–2598, Oct 2008.

[9] W. Li, L. Vanfretti, and J. H. Chow, "Pseudo-Dynamic Network Modeling for PMU-Based State Estimation of Hybrid AC/DC Grids," *IEEE Access*, vol. 6, pp. 4006–4016, 2018.

[10] P. Kokotovic, H. K. Khali, and J. O'reilly, *Singular perturbation methods in control: analysis and design*. Siam, 1999, vol. 25.

[11] I. Ivanov and A. Murzin, "Optimal filtering of synchronized current phasor measurements in a steady state," in *2015 IEEE International Conference on Industrial Technology (ICIT)*, March 2015, pp. 1362–1367.

[12] W. Li, M. Wang, and J. H. Chow, "Fast event identification through subspace characterization of PMU data in power systems," in *2017 IEEE Power Energy Society General Meeting*, July 2017, pp. 1–5.

[13] R. E. Skelton, "Dynamic systems control: linear systems analysis and synthesis," *Synthesis*, vol. 1500, p. 23946, 1988.